IET Science, Measurement & Technology

Research Article

IET Journals
The Institution of Engineering and Technology

Influence of temperature on interfacial charge of power transformer insulation

ISSN 1751-8822
Received on 14th December 2018
Revised 23rd May 2019
Accepted on 20th June 2019
E-First on 25th July 2019
doi: 10.1049/iet-smt.2018.5668
www.ietdl.org

Saurabh Dutta[1] ✉, Deepak Mishra[1], Nasirul Haque[2], Arpan Kumar Pradhan[2], Arijit Baral[1], Sivaji Chakravorti[2]

[1]*Department of Electrical Engineering, Indian Institute of Technology (ISM), Dhanbad, India*
[2]*Department of Electrical Engineering, Jadavpur University, Kolkata, India*
✉ *E-mail: dutta.saurabh2@gmail.com*

Abstract: One of the popular methods for insulation diagnosis is measurement and analysis of polarisation–depolarisation current (PDC). During normal operation, charges get confined at the interface of oil–paper insulation. A part of these accumulated charges get absorbed in depolarisation current and contribute to the overall PDC data. The process through which charges are released from their confinement is known as charge de-trapping, which is highly influenced by thermal energy content of the insulation and hence by measurement temperature. In the current work, an effort has been made to investigate the effect of measurement temperature on de-trapped charge. Two samples are prepared and analysed in the laboratory at different temperatures for this purpose. This is followed by analysis of data collected from several real-life power transformers. Related analysis presented here suggests that measurement temperature of the system plays an important role in determining the amount of de-trapped interfacial charge during PDC measurement.

1 Introduction

On application of a charging voltage across an initially relaxed dielectric, different polarisation processes get initiated within it. These polarisation processes include fast (electronic and ionic) as well as slow (dipolar) polarisation. Out of these processes, electronic and ionic polarisation phenomena are not affected by measurement temperature. In polarisation–depolarisation current (PDC) measurement technique, current measurement is not initiated simultaneously with voltage application but after a small time delay. This is done to avoid the influence of transients [1] in the recorded data. This implies, current measured during polarisation phase of PDC measurement is affected by only slow dipolar polarisation and constant leakage or conduction current of the insulation. It is worth mentioning here that henceforth, in the paper the term '*polarisation current*' is used to represent this current that is recorded during polarisation phase of PDC measurement.

In any dielectric, dipolar polarisation and leakage current magnitude are influenced by measurement temperature. With increase in temperature, the bonds present in the insulation matrix gets weaker [2]. Due to weakening of these bonds, energy required for freeing charge from the insulation matrix reduces. This in turn leads to increase in dc conductivity of the insulation [2]. Increase in measurement temperature leads to availability of excess thermal energy which increases the mobility of charge carriers [3]. Furthermore, increase in measurement temperature reduces the overall dipole orientation time. These factors lead to reduction of time required for completing the polarisation process within the insulation. The above discussion suggests that the profile of polarisation current is sensitive to measurement temperature.

It is generally assumed that profile of polarisation current (after removing the conduction current) at a given temperature will be similar to that of the depolarisation current [1]. However, there exists some difference between these two currents, particularly in aged transformers. In previous investigations by some of the authors it was revealed that this difference can be explained through the presence of charge de-trapping current present in depolarisation current [4, 5]. This current originates due to the absorption of a part of the accumulated ionic charge in oil–paper interface region through the transformer bushings and windings acting as electrodes during PDC measurement. The primary reasons behind the accumulation of this interfacial charge are conductivity difference between oil and paper, and presence of aging by-products which act as source of ionic charge carriers. Relative motion between solid and liquid during oil-circulation [6] leads to double layer [7] formation and subsequence charge separation at the interface. Cellulosic (or paper) part has high affinity towards negatively charged ions and has a tendency to adsorb impurities from oil. These adsorbed impurities act as trap sites for charge carriers [6]. However, positive charge carriers which remain in the oil get ultimately neutralised by the formation of streaming current [8] due to oil-circulation. This suggests that trapped charge carriers remain adsorbed to the paper surface at the oil-paper interface until they acquire sufficient energy to free themselves.

The ionic charge carriers present in the interfacial region will inarguably polarise molecules and dipoles in its surrounding. This creates a screen of dipoles surrounding the ion, producing a potential barrier or ion trap hindering the motion of the ion [9]. The ion requires sufficient energy to overcome this trap which it normally obtains through thermal vibrations. The ions which are able to escape or 'de-trap' from the ion trap during depolarisation current measurement contribute a significant part in the measured depolarisation current, particularly for aged and moisture-prone transformers.

The above discussion suggests that if an assessment of the freed interfacial charge can be made from PDC measurements, it can be beneficial for condition monitoring purpose. As trapped charges get released only after absorbing trap energy in the form of thermal oscillations [4], it is understood that influence of temperature (at which PDC measurement is carried out) on de-trapped charge need to be studied in detail. This paper focuses on investigating the effect of measurement temperature on the magnitude of total de-trapped charge. In the present work, PDC data, recorded from laboratory samples, at different temperatures are analysed first. Thereafter, this analysis is extended to PDC data recorded (at different measurement temperatures) from several in service power transformers. Details of the transformers along with the PDC measurement temperatures are given in Table 1. It is worth mentioning here that the two PDC measurement data of Trf8

Table 1 Details of transformers used

Transformer name	Power rating	Age of operation (in years)	Meas. temp., °C
Trf1	420 kV/240 MVA	36	30.1
Trf2	400 kV/240 MVA	33	29.8
Trf3	420 kV/200 MVA	28	30.1
Trf4	420 kV/200 MVA	28	30.0
Trf5	420 kV/200 MVA	28	29.8
Trf6	420 kV/240 MVA	20	30.8
Trf7	290 kV/230 MVA	35	30.1
Trf8	400 kV/240 MVA	29	30.0, 39.0
Trf9	400 kV/240 MVA	31	41.8
Trf10	420 kV/200 MVA	31	38.0
Trf11	420 kV/200 MVA	29	35.0
Trf12	166 kV/230 MVA	30	25.0

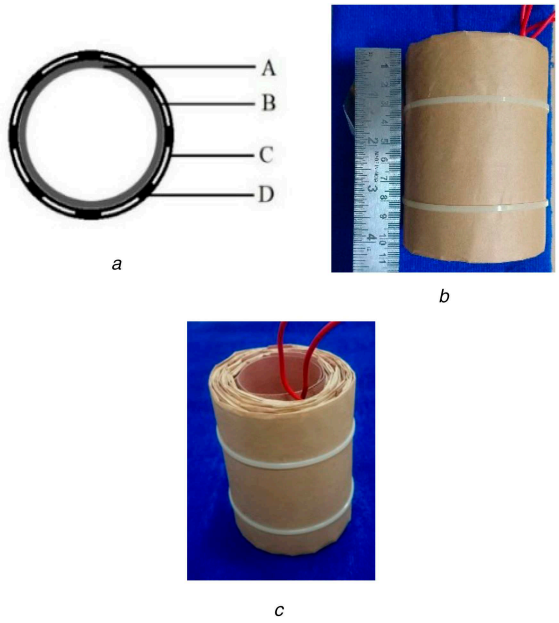

Fig. 1 *Sample construction*
(a) Schematic top view of sample constructed (A) Pressboard cylinder (B) Copper foil wrapped with Kraft paper (C) Wrapped copper foil (D) Pressboard strip; ***(b)*** Side view of the constructed sample; ***(c)*** Completed sample

Fig. 2 *Oil impregnation setup*
(A) Steel container containing oil-paper sample ***(B)*** Glass chamber (C and D) Valves ***(E)*** Manual vacuum pump ***(F)*** Pump ***(G)*** Bottle containing silica gel ***(H)*** Flow-meter

(mentioned in Table 1) are taken one month apart. It is assumed that the insulation of Trf8 did not undergo significant aging between these two measurements. Further, to show the capability of de-trapped charge (after proper normalisation) to act as a performance parameter, its variation with tanδ (dissipation factor) and Z_1 (highest magnitude of zero computed from transfer function of insulation model) are reported in this paper. Related analysis presented in this paper suggests that there is a well-defined relationship between the variation in de-trapped charge magnitude and measurement temperature. Application of this relationship can largely mitigate the effect of temperature, thus enhancing the effectiveness of normalised de-trapped charge as a performance parameter for power transformer insulation.

2 Sample construction

Two structurally identical samples were constructed in the laboratory for the present work: Sample1 using new Kraft paper and pressboard; Sample2 using old Kraft paper and pressboard that were available at the laboratory. This was done to emulate new (un-aged) and old (degraded) cellulosic insulation. Furthermore, forced oil circulation was implemented for a fixed duration so that trapped charges get introduced at the interface [6]. Figs. 1*a–c* depict the schematic diagram, side view and completed sample, respectively. The construction of the sample starts with a 2-mm-thick pressboard cylinder (A) with height 10 and 5 cm diameter. This cylinder forms the inner support of the sample. To emulate low-voltage and high-voltage windings, two copper foils (B and C) wrapped with 2 mil Kraft paper were rolled over A. To emulate spacers, 8 (1.5-cm-wide and 2-mm-thick) pressboard strips (D) were uniformly placed between B and C.

Post construction, the samples were heated at 80°C for several days in the hot air oven [5] for drying purposes. It was verified that after the heating period was over, the dryness of the samples were within acceptable limit. After drying, the two samples (Sample1 and Sample2) were weighed using a precision weighing scale and exactly 2% moisture (by cellulose weight) was allowed to be absorbed by both Sample1 and Sample2. Each sample was thereafter placed inside a sealed steel container containing 1.5 litres of mineral oil for impregnation. Old mineral oil was used for preparation of the samples. The moisture content of the mineral oil was observed (measured using Doble Domino) to be 16 ppm. Fresh oil was not used in the present work for two reasons: First, flow electrification-related problems are prominent in aged transformers which is likely to have old mineral oil. Thus, use of old impure mineral oil tends to emulate practical scenario. Second, flow electrification and associated charge separation at the interface [6] is augmented by oil impurities and hence is worth studying.

The oil impregnation process was performed using setup shown in Fig. 2. The setup is constructed to ensure oil impregnation of sample can be carried out in a dry environment. This further ensures that no excess moisture from the atmosphere is absorbed by oil volume during impregnation process. In Fig. 2, dry sample immersed in mineral oil (marked as A) was placed inside the glass chamber, B for impregnation. This glass chamber was fitted with two valves (C) and (D). Valve (C) was connected to a manually operated vacuum pump, E. While, valve D was connected to an air pump (F) via a glass bottle containing silica gel, G. With (C) open and (D) closed, the vacuum pump was operated. Once sufficient low pressure inside the glass chamber was achieved using vacuum pump (E), valve (C) was closed and D was opened. Thereafter, air pump (F) was used to fill the chamber with air. The air from the pump, (F), was passed through silica gel to ensure only de-moisturised air was used to fill the glass chamber. A flow-meter, H, was used to monitor the flow rate of the de-moisturised air during this tenure. Holes present on top of the steel container, (which were later used for connecting leads to the sample) enabled replacement of moist air within the steel container with de-moisturised air. After impregnation when the sample is connected with the PDC equipment using suitable leads these holes get automatically blocked.

Every 3 to 4 h, the air inside the glass chamber was replaced with a fresh volume of de-moisturised air. This process of

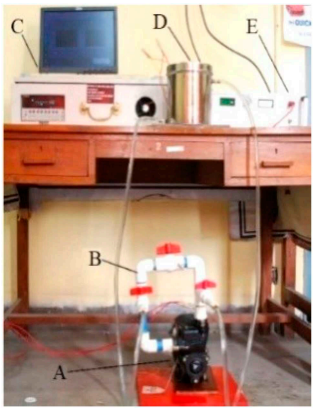

Fig. 3 *Experimental setup for recording PDC of test sample containing de-trapped charge.*
(A) Oil circulation pump, ***(B)*** Oil flow speed control circuit ***(C)*** PDC measuring equipment, ***(D)*** Steel container containing Sample, ***(E)*** DC voltage source

removing air and introduction of de-moisturised air into chamber B was done to ensure that air above the sample during impregnation remains always dry. It is reported in [10] that absorption of moisture by oil from atmosphere becomes effective only with sufficient agitation of oil volume [10]. Hence, care is taken not to disturb the steel can containing the oil-immersed paper sample during the impregnation process.

It is reported in [11] that oil impregnation and associated moisture equilibrium for laboratory sample can be achieved after 7 days. Consequently, in the present work, the above mentioned oil-impregnation process was continued for 8 days. Post-impregnation, the paper moisture in Sample1 and Sample2 were found (measured using IDAX300) to be 2.1 and 2.3%, respectively. After the oil–paper impregnation process was completed, the sealed steel container containing the sample was transferred to the oil-circulation setup.

For PDC measurement, a setup designed and constructed at High Tension Laboratory of Jadavpur University was used (shown in Fig. 3). Forced oil circulation was implemented with the help of oil flow control circuit shown as A and B in Fig. 3. In real-life transformers, charge separation at the interface is primarily generated due to relative movement between oil and paper. This oil flow can be either due to natural convection process or due to forced circulation. It is understood that more the tenure of oil-circulation, larger will be the quantity of charge deposited at the interface [6]. In the case of laboratory sample, forced circulation is opted to implement relative movement between oil and paper surface. This is done so that charge separation can happen at the interface of the sample. Furthermore, to ensure sizeable amount of charge trapping (sufficient for affecting the profile of PDC data), the oil-circulation was continued for long period (96 h). Post oil circulation, PDC measurement was carried out at different temperatures (40, 50 and 60°C). This was made possible by keeping the oil-immersed samples with oil circulation circuit inside heating chamber at constant temperature for several days [12] prior to PDC measurement at each temperature.

3 Identification of de-trapping current

Linear dielectric theory assumes that dielectric current, i_{dielec} that flows through the insulation on application of charging voltage is given by (1a). In (1a), i_{cond} represents the contribution of conduction or leakage current, whereas i_p can be given by (1b).

$$i_{\text{dielec}} = i_p + i_{\text{cond}} \tag{1a}$$

$$i_p = i_{\text{absorption}(p)} + i_{\text{displacement}} \tag{1b}$$

where $i_{\text{displacement}}$ is due to ionic and electronic polarisation while $i_{\text{absorption}(p)}$ is due to dipolar polarisation (dipole relaxation). Ionic and electronic polarisation being fast phenomenon [13], usually get completed within a very short time frame. It is a known fact that during PDC measurement, current measurement is not initiated immediately after charging voltage is applied. A small time delay is introduced in the current measurement process to avoid the influence of transients [14] in the recorded current data. As a result, current recorded during Polarisation phase of PDC measurement get affected by only slow dipolar polarisation phenomenon and constant leakage current with minimal or no influence of $i_{\text{displacement}}$ current.

During the depolarisation phase, when the terminals of the test object are short-circuited, dipoles (in absence of field) get relaxed and release their dipole energy obtained during polarisation phase. It is a general practice to assume that depolarisation current (i_d) is generated due to relaxation of dipoles, $i_{\text{absorption}(d)}$ only and is given by (2).

$$i_d = i_{\text{absorption}(d)} \tag{2}$$

There are two ways by which charge build-up can happen at the oil-paper interface: Through charge injection and through ionisation or charge separation [15]. It is known from [13] that the charging voltage for PDC measurement for transformer must not exceed 1000 V as this may introduce non-linearity in the system. For charge injection (during the excitation period), around 10 kV/mm threshold field is required [16]. As the excitation voltage applied during polarisation is less than or equal to 1000 V, charge injection during polarisation phase is unlikely. As a result, only the dielectric medium gets ionised due to the test voltage applied during polarisation phase. In a power transformer, availability of a large number of oil-paper layers constitute a large interfacial region [17, 18]. At microscopic level, there exists a large amount of broken bonds [15], forming trap sites for charge carriers and over time result in charge accumulation at the interfacial region.

It is explained in [19, 20] that a classical two potential well model can be used to explain the process of ion conduction in a typical solid-liquid insulation system. According to the model, the ionic conduction takes place as the trapped ions move from one site to the other. Assuming that there exists two close-by trap sites, ts1 and ts2, separated by a distance $2a$ and a barrier energy of ΔH_b. Sufficient energy required for an ion located at ts1, jump to ts2, under applied electric field E_f, is $(\Delta H_b - \text{qaE}_f)$, where q is the charge of the ion. Likewise, the energy required for charge to jump from location ts2 to ts1 is $(\Delta H_b + qaE_f)$ [19]. If the external field is absent, the probability of an ion to move from ts1 to ts2 can be given by (3) [19].

$$P = f_v \exp\left[-\frac{\Delta H_b}{k_c T}\right] \tag{3}$$

where, f_v is the frequency of vibration (number of ion jumps attempted per unit time), k_c is the Boltzmann's constant (1.38×10^{-23}) and T is the temperature. It is reported that value of f_v lies typically in the range of 10^{11} to 10^{12} [21]. The relaxation time, τ_r of this process can be expressed in terms of P as given by (4).

$$\tau_r = \frac{1}{2P} \tag{4}$$

Depending upon the availability of trap energy, charge can take hours to de-trap from the trap site [5]. It is reported in [16, 22] that this de-trapping time of charge is less in oil–paper insulation as compared to polymers. These de-trapped charges reach the electrodes to get neutralised and this result in a current flow. This de-trapping current contributes to the depolarisation current. It is reported that separation of de-trapping current and the relaxation current from depolarisation current is possible provided some assumptions are made [4]. In order to improve readability these assumptions are re-iterated as follows:

(i) No charge has been injected into the insulation during polarisation period from electrodes [4].

(ii) The oil–paper insulation system is heterogeneous and contains several types of dipoles such as oil, paper, and water dipoles. Considering same period for polarisation and depolarisation, the dipole current contribution amid both these stages for a specific dipole group will be same.

The de-trapping current can be calculated by eliminating the current component due to the relaxation of dipoles from the depolarisation current given in (5) [4].

$$i_d = i_{\text{absorption}(d)} + i_{\text{de-trap}} \tag{5}$$

where $i_{\text{de-trap}}$ is the current flowing due to de-trapping of trapped charges. For a similar $i_{\text{absorption}(d)}$ contribution in i_p and i_d, $i_{\text{de-trap}}$ is related to i_p and i_d using (6)

$$i_p - i_d = i_{\text{cond}} - i_{\text{de-trap}} \tag{6}$$

The conduction current in (6) can be obtained by adding the steady state values of polarisation current and depolarisation current given by (7).

$$i_{\text{cond}} = |i_p(t_{\text{ss}})| + |i_d(t_{\text{ss}})| \tag{7}$$

where, $|i_p(t_{\text{ss}})|$ and $|i_d(t_{\text{ss}})|$ represent the absolute values of steady state polarisation current, i_p and depolarisation current, i_d, respectively. Available literature suggests that the de-trapping current can be characterised by a single exponentially decay function [23, 24]. Hence, the de-trapping current, $i_{\text{de-trap}}$ in the present paper is approximated by (8).

$$i_{\text{de-trap}} = A \times \exp(-t/) \tag{8}$$

Here, A is the initial value of de-trapping current, t is the time and ς is the time constant of the de-trapping current.

4 Effect of measurement temperature on trapped charge

It has been already mentioned that the energy gained by trap charge is mostly obtained in the form of thermal oscillations [25]. This implies that a variation in PDC measurement temperature and hence change in thermal energy content of the insulation system influences the charge de-trapping process. As PDC measurement temperature of the system is increased, more thermal energy becomes available to the trapped charge. This suggests that the increase in measurement temperature has direct influence on the result obtained during depolarisation current measurement. The following segment details the effect of measurement temperature on the de-trapped charge as observed in the case of laboratory sample and in-service transformers.

4.1 Laboratory sample

For PDC measurement at different temperatures, a temperature controlled hot air oven was used to maintain the temperature constant for a given sample. In the case of the laboratory samples, PDC measurement was carried out at 40, 50, and 60°C. It is worth mentioning here that prior to PDC measurement, all the samples were allowed to attain thermal equilibrium by keeping them at constant temperature for several days [11]. Figs. 4*a* and *b* show the polarisation and depolarisation current profile obtained for Sample1 at different temperatures. As the excitation field was much <10 kV/mm, there was no possibility of charge injection during this period [25], and the current recorded was only due to dipole excitation and dc conduction. Hence, after eliminating the conduction current from the polarisation current, only the dipole excitation current part remains [4]. Current $i_{\text{de-trap}}$ calculated at different temperatures using (7) and (8) for *Sample*1 (at different temperatures) are shown in Fig. 4*c*. These profiles of $i_{\text{de-trap}}$ were further used to calculate the total charge de-trapped from the interfacial region at a given measurement temperature. Amount of

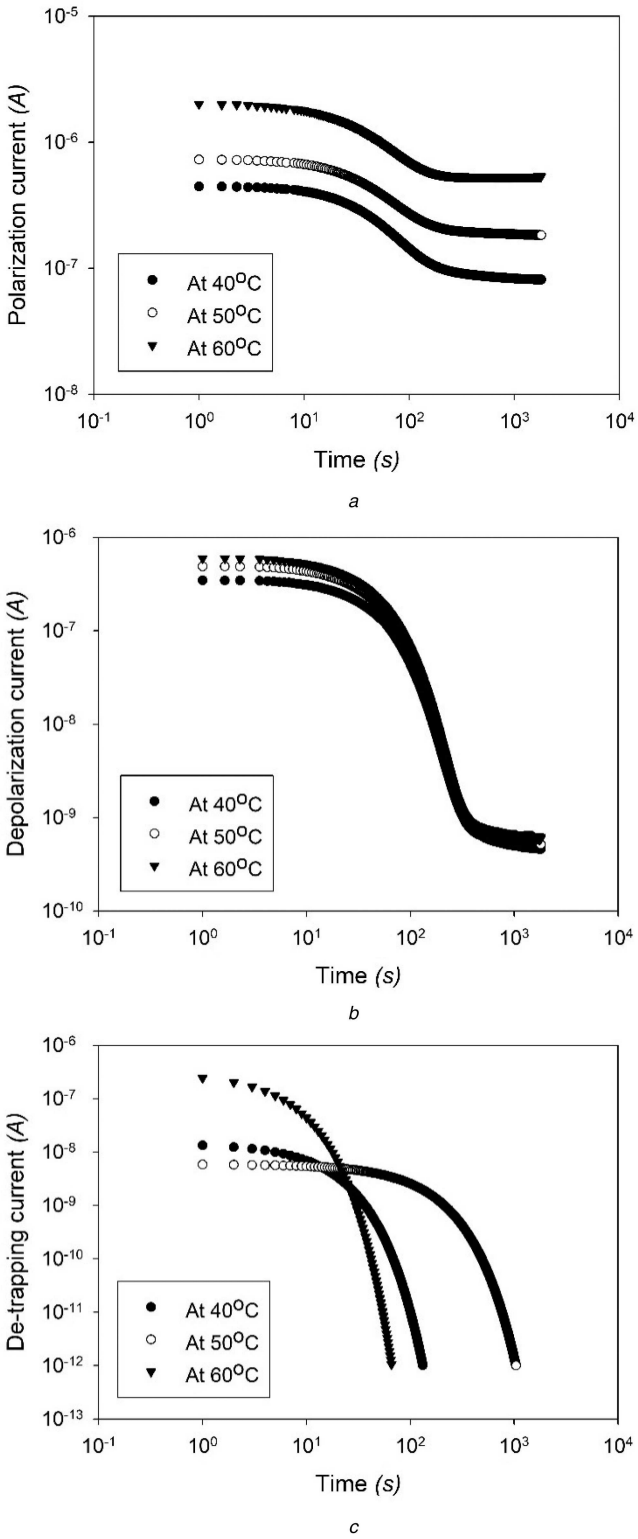

Fig. 4 *Current responses for Sample1 at different temperatures*
(a) Polarisation current profile for Sample 1 at different temperatures, ***(b)*** Depolarisation current profile for Sample 1 at different temperatures, ***(c)*** De-trapping current obtained for Sample 1 at different temperatures

charge, Q_d de-trapped during depolarisation current measurement can be obtained from $i_{\text{de-trap}}$ using (9) [4].

$$Q_d = \int i_{\text{de-trap}} \mathrm{d}t \tag{9}$$

The above procedure of obtaining Q_d was applied to PDC data obtained for both samples at different temperatures. It can be easily understood that the magnitude Q_d is sensitive to insulation

geometry and applied voltage during polarisation process. A larger insulation geometry implies more interface regions, therefore, higher amount of Q_d. Similarly the ionic conduction process responsible for charge accumulation is influenced by applied electric stresses. As the insulation geometry and size for both the insulation samples are almost same, the magnitude of de-trapped charge obtained from them can be readily compared. However this assumption fails for real power transformers, which vary in insulation geometry and size. Therefore, to facilitate comparison of de-trapped charge (calculated from PDC measurements conducted on two different insulation systems), Q_d is normalised by the product of geometric capacitance and charging voltage, (C_0U_0) taking account for both the influence of insulation geometry and applied voltage.

During measurement of PDC data from samples, the charging voltage U_0 was considered to be 250 V. Normalised de-trapped charge $(Q_{\text{norm}} = (Q_d/U_0C_0))$ corresponding to different measurement temperatures for Sample1 and Sample2 are given in Table 2. It is worth mentioning here that capacitance of test samples were measured using Nvis 9304T LCR meter. It can be seen from Table 2 that the overall trend of the normalised de-trapped charge is to increase with increase in measurement temperature. Furthermore, the rate of increase in Q_{norm} is larger for sample constructed using old (degraded) paper. This happens because abundance of thermal energy at elevated temperature invariably leads to increased number of charge de-trapping. Another noteworthy point is that at higher temperatures, the difference of conductivity between oil and paper widens [6, 26]. This facilitates more accumulation of charge in the interface regions, hence more amount of charge de-trapping. Further, variation of time constant with temperature is given in Table 3. In the case of de-trapping current, time constant represents the time required for the trapped charge to get de-trapped from the interface. Hence, time constant of de-trapping current not only depends on temperature, but also on trap depth. In the case of samples, Sample1 has been prepared using new Kraft paper whereas the Sample2 has been prepared using old Kraft paper. Time constant for Sample2 is observed to be significantly higher than Sample1. This signifies, trapped charge carriers in Sample2 take significantly longer time to free themselves. This is a characteristic of deep traps. The presence of deeper trap depth in Sample2 is due to use of old and degraded Kraft paper in the construction of Sample2. This further suggests that the time constant not only depends upon the measurement temperature but also on the trap depth at the interfacial. Hence, despite of having similar construction and measurement temperature, the variation of time constant with temperature is incapable of providing meaningful results due to the presence dissimilar trap depths.

4.2 In-service power transformer

As the temperature of the insulation system increases, the performance parameters tanδ and Z_1 (zero of the transfer function of CDM having the highest magnitude) also increases [27]. This information coupled with the general trend of normalised de-trapped charge with temperature (indicated by Table 2) suggests that normalised de-trapped charge can also be considered as an important performance parameter. To support the above hypothesis, tanδ and Z_1 corresponding to a number of real life transformers (Trf1 to Trf7) were compared with their corresponding normalised de-trapped charge. At this stage, only Trf1 through Trf7 are used as the PDC measurement temperature of these units are nearly constant. The procedure explained in previous section is used to evaluate normalised de-trapped charge at 30°C for the transformers Trf1 to Trf7. The values of Q_{norm}, %tanδ and Z_1 obtained for transformers Trf1 to Trf7 are mentioned in Table 4. Variation of %tanδ with normalised de-trapped (Q_{norm}) obtained for these units are shown in Fig. 5*a*. The fitted curve shown in Fig. 5*a* is observed to have a form given in (10).

$$\tan\delta = y_0 + (a_1) \times (1 - \exp(-b_1 \times Q_{\text{norm}})) \tag{10}$$

Table 2 Variation of normalised de-trapped charge w.r.t. temperature for Sample1 and Sample2

Temperature, *T*, °C	Q_{norm} for *Sample*1	Q_{norm} for *Sample*2
40	0.0167	0.0514
50	0.0537	0.1301
60	0.1069	0.3186

Table 3 Variation of time constant for Sample1 and Sample2

Temperature, T, °C	Time constant for *Sample*1	Time constant for *Sample*2
40	21.81	388.83
50	15.57	238.42
60	6.26	43.86

Table 4 Normalised de-trapped charge and their corresponding tanδ and zero of in-service transformers

Transformer name	Q_{norm}	tanδ	Zero
Trf1	18.14	0.48	5.25
Trf2	5.82	0.41	1.59
Trf3	2.65	0.13	0.62
Trf4	5.63	0.37	0.64
Trf5	3.53	0.14	0.50
Trf6	4.26	0.34	0.44
Trf7	12.71	0.43	4.72
Trf8	2.50	0.16	0.55

The value of coefficients (y_0, a_1, b_1) in (10) are found to be (−0.49, 0.95, 0.40), respectively. A similar nature was observed between Q_{norm} and Z_1 as illustrated by Fig. 5*b*. It is observed that the data in Fig. 5*b* maintain a relationship given in (11)

$$Z_1 = a_2/(1 + \exp(-(Q_{\text{norm}} - b_2)/c_2)) \tag{11}$$

The value of coefficients (a_2, b_2, c_2) in (11) are found to be (5.28, 2.22, 7.85), respectively. It is understood from Figs. 5*a* and *b*, that magnitude of normalised de-trapped charge maintains a good correlation with performance parameters like tanδ and Z_1. This once again suggests that the normalised de-trapped charge can indeed be considered as a performance parameter for in-service power transformers. However, care should be taken as these relations ((10) and (11)) are valid for 30°C only.

During field measurement of PDC data, it is practically difficult to ensure that the measurement temperature will be maintained at 30°C for all transformers. Hence, scope of applying (10) and (11) in their current form are rather limited. This issue can be addressed by considering the influence of measurement temperature in (10) and (11).

In order to address this issue, data collected from Trf8 through Trf12 were used. As shown in Table 1, PDC data for Trf8 (data corresponding to 40°C) to Trf12 were recorded at temperature other than 30°C. Table 5 shows the normalised de-trapped charge obtained for the above referred transformers at temperatures other than 30°C. It is worth mentioning here that PDC data collected from Trf8 at 30°C is not used at this stage. Later in the paper PDC data of Trf8 measured at 30°C is used for validation purposes. The de-trapping current profiles obtained for transformers (Trf8 to Trf12) are illustrated in Fig. 6*a*. Fig. 6*b* shows the variation of time constants with temperature corresponding to different transformers. The time constant (ς) in (8) represents the time taken by trapped charge (located at a specific trap depth) to gain required energy to free itself.

Variation in measurement temperature leads to variation in thermal energy content of the insulation. Hence, the value ς is likely to be different for a given carrier (located at a specific trap depth) at different temperatures. Also, different trap charges are

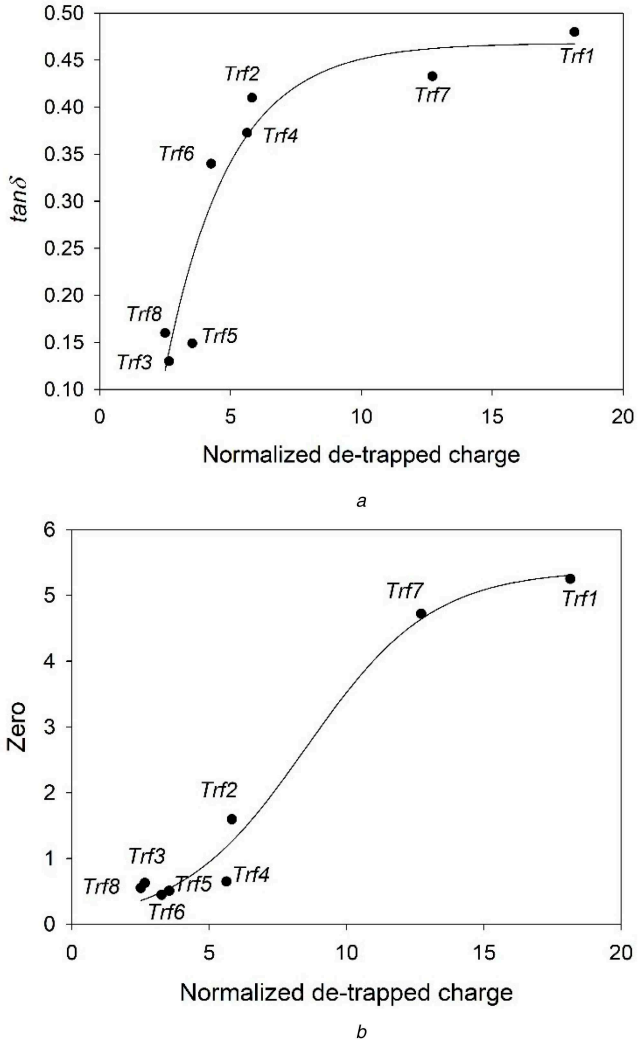

Fig. 5 *Variation of normalised de-trapped charge with insulation sensitive parameters*

(a) Variation of tan delta with normalised de-trapped charge, ***(b)*** Variation of zero with normalised de-trapped charge

Table 5 Normalised de-trapped charge in tested transformers at different temperatures

Transformer name	Meas. temp., °C	ΔT, °C	Normalised de-trapped charge	Time constant ς, s
Trf8	39	14	4.50	231.66
Trf9	42	17	4.90	86.20
Trf10	38	13	3.16	1428.57
Trf11	35	10	2.57	588.23
Trf12	25	0	1.89	138.88

located at different trap depths and hence require different energy to free itself [24, 25]. Deeper the trap, larger is the energy required by the trapped charge to free itself and hence longer is the time required. Increase in measurement temperature means availability of increased thermal energy. Hence, increase in measurement temperature should reduce the time constant. However, it can be observed from Fig. 6*b* that there is no co-relation between time constants (obtained from different transformer) and temperature. This can be explained by the fact that time constant is dependent on the surface condition, total surface area of the insulation and availability of sufficient energy (i.e. trap energy). Since, different units have different insulation dimension, having dissimilar trap depths, comparison of time constants (without normalisation) corresponding to different transformers does not provide meaningful and usable results. This further shows that the

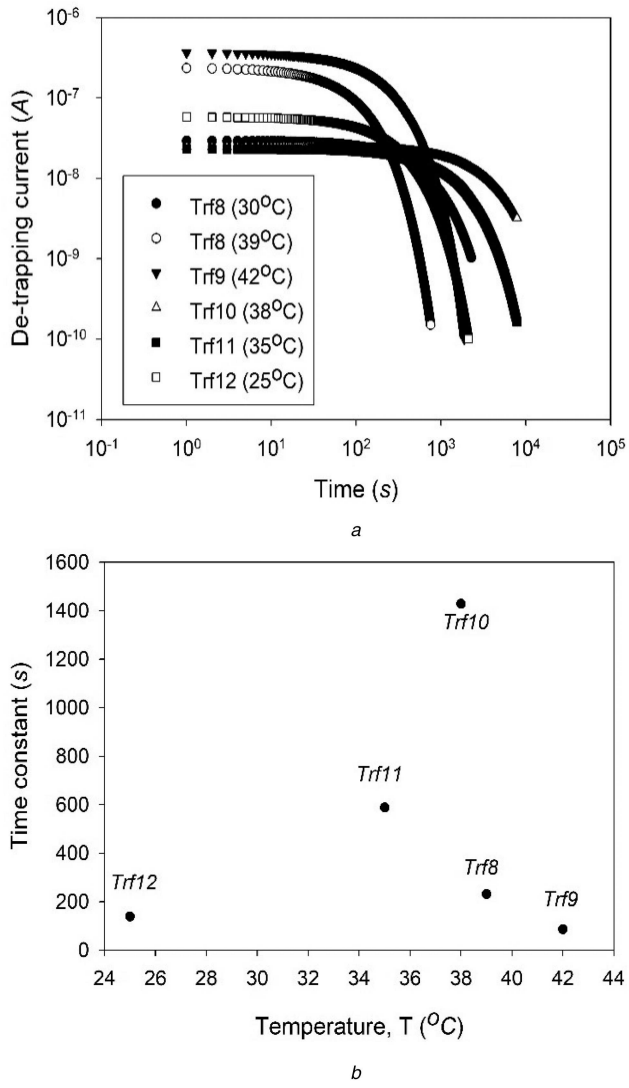

Fig. 6 *Variation of de-trapping current and their corresponding time constant with temperature*

(a) De-trapping current obtained from a number of transformers with temperature, ***(b)*** Variation of time constant with temperature

normalised de-trapped charge might be more useful in comparison to the time constant for detecting insulation condition.

It is understood that value of normalised charge (indicated by Table 5) is influenced by PDC measurement temperature. Furthermore, normalisation of de-trapped charge effectively reduces the influence of insulation geometry. Hence, data presented in Table 5 can be successfully compared to decipher the influence of measurement temperature on normalised de-trapped charge. Fig. 7 shows the variation of normalised de-trapped charge with change in measurement temperature, ΔT (taking 25°C as reference temperature) that was observed for transformer Trf8 to Trf12.

To model the variation in normalised de-trapped charge with respect to temperature, a parameter $\delta Q_{\text{norm\_var}}$ (given by (12)) is introduced.

$$\delta Q_{\text{norm\_var}}(T_1) = (Q_{\text{norm}}(T_1) - Q_{\text{norm\_25}})/Q_{\text{norm\_25}} \tag{12}$$

In (12), $Q_{\text{norm}}(T_1)$ is the measured normalised de-trapped charge at any given temperature T and $Q_{\text{norm\_25}}$ is the measured normalised de-trapped charge at 25°C. It is understood that for Trf12, the values of $\delta Q_{\text{norm\_var}}$ and ΔT will be zero, as the PDC measurement temperature was 25°C. The calculated values of $\delta Q_{\text{norm\_var}}$ are now plotted against ΔT Fig. 8, where ΔT is the difference between measurement temperature and 25°C. It has been already discussed that the normalised de-trapped charge is not influenced by insulation geometry. The above discussion suggests that Q_{norm} of

*Trf*8 to *Trf*12 mentioned in Table 5 can be thought as normalised de-trapped charge measured from units having identical insulation condition at different temperatures ranging from 25 to 42°C. It is found that (13) is capable of modelling the relationship that exists between $\delta Q_{\text{norm\_var}}$ and ΔT.

$$\delta Q_{\text{norm\_var}}(\Delta T) = y_0 + a\Delta T^b; \quad \Delta T = T - 25 \tag{13}$$

The values of y_0, a and b in (13) are found to be −0.0280, 0.0012, and 2.5815, respectively. It is noteworthy that (13) attempts to model the change in Q_{norm} bought by temperature, and not Q_{norm} itself. If the values of Q_{norm} and $\delta Q_{\text{norm\_var}}$ at $T_1(\neq 25°\text{C})$, are known, then the value of Q_{norm} at any given temperature $T_2(\neq T_1)$ can be obtained using (12) and (13). The steps involved in predicting $Q_{\text{norm}}(T_2)$ are detailed below,

Step 1: The value of $\delta Q_{\text{norm\_var}}$ at T_1 is first evaluated using (13). Then using expression (12), the value of $Q_{\text{norm\_25}}$ is calculated.
Step 2: Now, the value of $\delta Q_{\text{norm\_var}}$ at T_2 is calculated using (13). Finally, $Q_{\text{norm}}(T_2)$ can be calculated using the following equation,

$$Q_{\text{norm}}(T_2) = Q_{\text{norm\_25}} \times (1 + \delta Q_{\text{norm\_var}}(T_2)) \tag{14}$$

It should be remembered here, for finding $\delta Q_{\text{norm\_var}}$ at T_1 and T_2, ΔT in (13) should be replaced by ΔT_1 and ΔT_2, respectively. The methodology described above can be highly beneficial for comparing the Q_{norm} values obtained from PDC measurements conducted on different transformers at various temperatures, thus eliminating the temperature effect on Q_{norm}. For this to happen, it is needed to confirm that the coefficients (13) are applicable to any power transformer, irrespective of size, shape and insulation status. The next section discusses the validation of the developed methodology.

5 Validation of the proposed methodology

In order to validate the proposed methodology, the value of $Q_{\text{norm}}(39)$ is predicted using $Q_{\text{norm}}(30)$ for Trf8. As $Q_{\text{norm}}(30)$ was not considered for identification of coefficients in (12) through (14) and PDC at two different temperatures are available for Trf8, such validation seems reasonable. The values of $Q_{\text{norm}}(39)$ obtained using recorded PDC data and using (14) along with the error involved in prediction are presented in Table 6. Table 6 shows that $Q_{\text{norm}}(39)$ can indeed be predicted from $Q_{\text{norm}}(30)$ with acceptable accuracy. Thus illustrating the fact that variation of Q_{norm} with temperature can be modelled using (12)–(14). It should be noted that the operational age of the transformers considered for Fig. 7 are almost same. Furthermore, the authors were informed by the utilities that all transformers considered in the work have operated at near full load capacity throughout their operational life. At the present moment, the authors do not have in their possession sufficient number of PDC data (recorded from transformers with age significantly different from 30 years) at different temperature. Consequently, variation of coefficients in (12)–(14) with operational age of transformers could not be reported in the present work. The authors are presently engaged in widening the PDC database. Once sufficient data become available, influence of transformer operational age on coefficients will be reported.

The laboratory samples used in the present work were carefully constructed so that the oil to paper ratio maintains a value that is generally observed for real-life transformers. Furthermore, normalisation of de-trapped charge (evaluated from PDC) effectively reduces the influence of insulation geometry. The above discussion suggests that the proposed method should be equally capable of modelling variation of Q_{norm} with ΔT for scaled down laboratory sample. Hence, the proposed methodology was applied on PDC data obtained from laboratory samples reported in Table 2. For each sample, the value of $Q_{\text{norm}}(40)$ was used for predicting $Q_{\text{norm}}(50)$ and $Q_{\text{norm}}(60)$ using (12) through (14). Thereafter, these predicted Q_{norm} values are compared with actual $Q_{\text{norm}}(50)$ and $Q_{\text{norm}}(60)$. Table 7 shows the result of such comparison. Tables 6 and 7 show that irrespective of difference in constructional complexity and size, prediction of $Q_{\text{norm}}(T_2)$ using $Q_{\text{norm}}(T_1)$ is indeed satisfactory for both scaled down laboratory samples as well as Trf8. In order to test the full potential of the developed method, $Q_{\text{norm}}(25)$ is predicted for all the tested transformers mentioned in Table 1. The second last column of Table 8 show the value of predicted $Q_{\text{norm}}(25)$. In order to improve readability, PDC measurement temperature (T_1) and $Q_{\text{norm}}(T_1)$ (evaluated from measured PDC) are also included in Table 8.

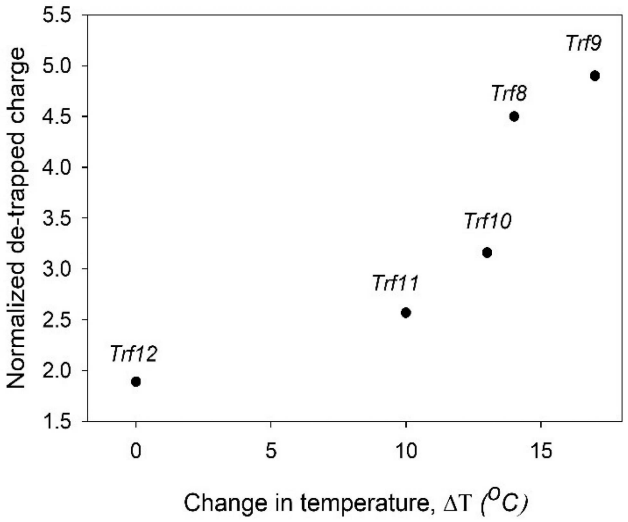

Fig. 7 *Variation of normalised de-trapped charge with change in measurement temperature*

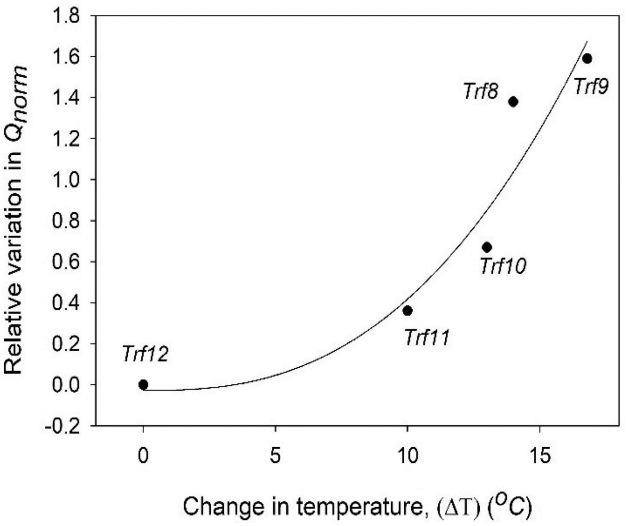

Fig. 8 *Change in δQ_{norm_var} with variation in measurement temperature and fitted curve according to (13)*

Table 6 $Q_{\text{norm}}(T_2)$ computed using PDC recorded at T_1

Transformer name	Temp., °C		$Q_{\text{norm}}(39)$		% error
	T_1	T_2	Using PDC	Using (14)	
Trf8	30	39	4.50	4.90	−8.88

Table 7 $Q_{norm}(T_2)$ computed using PDC recorded at T_1 for test samples

Sample name	Temp., °C		$Q_{norm}(T_2)$		% error
	T_1	T_2	Using PDC	Using (13)	
*Sample*1	40	50	0.05	0.04	20.00
	40	60	0.11	0.09	18.18
*Sample*2	40	50	0.13	0.14	−7.69
	40	60	0.32	0.29	−9.37

Table 8 Application of (13) in power transformers

Transformer name	T_1, °C	$Q_{norm}(T_1)$ (measured)	$Q_{norm}(25)$ (predicted)	ΔQ_{norm}[a]
*Trf*1	30.1	18.14	17.23	0.91
*Trf*2	29.8	5.82	5.59	0.23
*Trf*3	30.1	2.65	2.52	0.13
*Trf*4	30.0	5.63	5.37	0.26
*Trf*5	29.8	3.53	3.39	0.14
*Trf*6	30.8	4.26	3.93	0.33
*Trf*7	30.1	12.71	12.08	0.63
*Trf*8	30.0	2.50	2.38	0.12
*Trf*9	41.8	4.90	1.80	3.1
*Trf*10	38.0	3.16	1.69	1.47
*Trf*11	35.0	2.57	1.80	0.77
*Trf*12	25.0	1.89	—	—

[a]$\Delta Q_{norm} = Q_{norm}(T_1) - Q_{norm}(25)$.

Table 8 shows that value of $Q_{norm}(T_1)$ for Trf4 and Trf9 are close to each other. Apparently, this suggests that the insulation condition of both these units have similar conditions. However, when adjustments for temperature were made, it is revealed that there exists a large gap between $Q_{norm}(25)$ values of both the units. This suggests that the insulation condition of Trf4 is much inferior to that of Trf9. This is indeed the case as the value of tanδ value of Trf4 and Trf9 are 0.37 and 0.23, respectively. This once again emphasises the fact that understanding the effect of measurement temperature on Q_{norm} is necessary before it can be used as an aging sensitive performance parameter.

Table 8 further shows that $Q_{norm}(25)$ for Trf9, Trf10, and Trf11 are close to each other which reflects their similar insulation condition status. On the other hand, $Q_{norm}(25)$ of Trf8 shows that its insulation has significantly deteriorated in comparison to Trf9, Trf10, and Trf11 even though all four transformers have almost same operational age. Among the tested transformers, Trf1 and Trf7 are operating for a longer duration. Hence, these units are expected to have larger $Q_{norm}(25)$. Furthermore, Table 8 shows that magnitude of $\Delta Q_{norm}(25)$ for Trf2, 3, 4, 5, 6, and 8 is less than those observed for Trf9, 10, and 11. This is expected as PDC measurement temperature of Trf2, 3, 4, 5, 6, and 8 (compared to Trf9, 10 and 11) are much closer to 25°C.

6 Conclusions

In the present work, effect of measurement temperature on the de-trapping of charge is studied. Related analysis presented in this paper shows that magnitude of charge increases with increase in measurement temperature. Based on the findings reported in the paper, the following conclusions can be made:

- De-trapping of charge is influenced by ageing, cellulosic condition and measurement temperature.
- $Q_{norm}(30)$ maintains a specific relationship with tanδ and Z_1 for PDC data recorded at 30°C.
- $Q_{norm}(T)$ follows a well-defined relationship with measurement temperature T.
- A relationship is proposed using which Q_{norm} at any given temperature T can be evaluated. This facilitates comparison of transformer insulations at a common reference temperature.
- The need of using insulation model can be eliminated if Q_{norm} is used for insulation diagnosis. Furthermore, all problems associated with use of available linear models can be avoided.

7 References

[1] Saha, T.K., Purkait, P.: 'Investigation of polarization and depolarization current measurements for the assessment of oil–paper insulation of aged transformers', *IEEE Trans. Dielectr. Electr. Insul.*, 2011, **11**, (1), pp. 144–153

[2] Koufakis, E.I., Halevidis, C.D., Polykrati, A.D., *et al.*: 'Calculation of the activation energy of oil–paper insulation in a distribution transformer', *IEEE Electr. Insul. Mag.*, 2012, **28**, (2), pp. 52–58

[3] Ma, Z., Liao, R., Zhao, X., *et al.*: 'Influence of temperature on polarization and depolarization current of oil–paper insulation'. 2012 Inter. Conf. High Volt. Engg. Appl., Shanghai, 2012, pp. 426–430

[4] Mishra, D., Haque, N., Baral, A., *et al.*: 'Assessment of interfacial charge accumulation in oil-paper interface in transformer insulation from polarization-depolarization current measurements', *IEEE Trans. Dielectr. Electr. Insul.*, 2017, **24**, (3), pp. 1665–1673

[5] Mishra, D., Haque, N., Baral, A., *et al.*: 'Effect of charge accumulated at oil–paper interface on parameters considered for power transformer insulation diagnosis', *IET Sci. Meas. Technol.*, 2018, **12**, (3), pp. 411–417

[6] Metwally, I.A.: 'Characterization of static electrification in power transformers', *IEEE Trans. Dielectr. Electr. Insul.*, 1996, **3**, (2), pp. 307–315

[7] Touchard, G., Romat, H.: 'Mechanism of charge formation in double layer appearing at an hydrocarbon liquid-metal interface', *J. Electrost.*, 1982, **12**, pp. 377–382

[8] Cabaleiro, J.M., Paillat, T., Moreau, O., *et al.*: 'Flow electrification of dielectric liquids in insulating channels: limits to the application of the classical wall current expression', *J. Electrost.*, 2008, **66**, (1–2), pp. 79–83

[9] Kao, K.C.: '*Dielectric relaxation in solids*' (Elsevier, USA, 2004), ch. 7

[10] Sokolov, V., Aubin, J., Davydov, V., *et al.*: 'Moisture equilibrium and moisture migration within transformer insulation systems'. CIGRE WG A2. 30, France, 2008, pp. 1–52

[11] Saha, T.K., Purkait, P.: 'Investigations of temperature effects on the dielectric response measurements of transformer oil–paper insulation system', *IEEE Trans. Power Deliv.*, 2008, **23**, (1), pp. 252–260

[12] Li, J., Zhang, Z., Grzybowski, S., *et al.*: 'A new mathematical model of moisture equilibrium in mineral and vegetable oil–paper insulation', *IEEE Trans. Dielectr. Electr. Insul.*, 2012, **19**, (5), pp. 1615–1622

[13] Zaengl, W.S.: 'Dielectric spectroscopy in time and frequency domain for HV power equipment, part I: theoretical considerations', *IEEE Electr. Insul. Mag.*, 2003, **19**, (5), pp. 5–19

[14] Joshi, A., Aaradhi, P.: 'Dielectric diagnosis of EHV current transformer using frequency domain spectroscopy (FDS) & polarization and depolarization current (PDC) techniques', *Int. J. Sci. Eng. Res.*, 2012, **3**, (11), pp. 1–11

[15] Wu, K., Zhu, Q., Wang, H., *et al.*: 'Space charge behavior in the sample with two layers of oil-immersed-paper and oil', *IEEE Trans. Dielectr. Electr. Insul.*, 2014, **21**, (4), pp. 1857–1865

[16] Tang, C., Chen, G., Fu, M., *et al.*: 'Space charge behavior in multilayer oil–paper insulation under different DC voltages and temperature', *IEEE Trans. Dielectr. Electr. Insul.*, 2010, **17**, (3), pp. 775–784

[17] Zhou, Y., Wang, Y., Li, G., *et al.*: 'Space charge phenomena in oil–paper insulation materials under high voltage direct current', *J. Electrost.*, 2009, **67**, (2), pp. 417–421

[18] Schmidt, W.: 'Electronic conduction processes in dielectric liquids', *IEEE Trans. Dielectr. Electr. Insul.*, 1984, **5**, (19), pp. 389–418

[19] Bartnikas, R.: 'Performance characteristics of dielectrics in the presence of space charge', *IEEE Trans. Dielectr. Electr. Insul.*, 1997, **4**, (5), pp. 544–557

[20] Bartnikas, R.: 'Dielectric losses in solid-liquid insulating systems – part I', *IEEE Trans. Electr. Insul.*, 1971, **EI-5**, (4), pp. 113–121; also Part II, 6, (1), pp. 14–21

[21] Watson, P.K.: 'The transport and trapping of electrons in polymers', *IEEE Trans. Dielectr. Electr. Insul.*, 1995, **2**, (5), pp. 915–924

[22] Wang, S., Zhang, G., Mu, H., *et al.*: 'Effects of paper-aged state on space charge characteristics in oil-impregnated paper insulation', *IEEE Trans. Dielectr. Electr. Insul.*, 2012, **19**, (6), pp. 1871–1878

[23] Mazzanti, G., Montanari, G.C., Alison, J.M.: 'A space-charge based method for the estimation of apparent mobility and trap depth as markers for insulation degradation-theoretical basis and experimental validation', *IEEE Trans. Dielectr. Electr. Insul.*, 2003, **10**, (2), pp. 187–197

[24] Chen, G., Xu, Z.: 'Charge trapping and detrapping in polymeric materials', *J. Appl. Phys.*, 2009, **106**, (12), p. 123707

[25] Zhou, T., Chen, G., Liao, R., *et al.*: 'Charge trapping and detrapping in polymeric materials: trapping parameters', *J. Appl. Phys.*, 2011, **110**, (4), p. 043724

[26] Saha, T.K., Purkait, P.: 'Effects of temperature on time-domain dielectric diagnostics of transformers', *Aust. J. Electr. Electron. Eng.*, 2004, **1**, (3), pp. 157–162
[27] Dutta, S., Mukherjee, M., Pradhan, A.K., *et al.*: 'Effect of temperature on condition assessment of oil–paper insulation using polarization-depolarization current'. 19th National Power System Conf. (NPSC), Bhubaneswar, 2016, pp. 1–5